Acta Astronautica 214 (2024) 545–552

Contents lists available at ScienceDirect

Acta Astronautica

journal homepage: www.elsevier.com/locate/actaastro

The capture of small near-Earth asteroids in a bound binary pair in Earth's orbit

Amirah R. Algethami [*,1], Colin R. McInnes [2], Matteo Ceriotti [3]

Space and Exploration Technology Group, James Watt School of Engineering, University of Glasgow, Glasgow, G12 8QQ, UK

ABSTRACT

Hill's approximation models the motion of two small masses gravitationally interacting with each other and perturbed by a large central body. An application of the model is employed in this paper to manoeuvre the relative motion of two asteroids by a small impulse to capture them in bound binary motion in Earth's orbit. The initial conditions prior to the capture manoeuvre are restricted in a parameter space termed the gateway region. The gateway region is produced by applying the constraint that the capture impulse is a real-valued function, and the zero-velocity curve closes, enveloping both asteroids. A full mission scenario is designed with three impulses. The first impulse transfers one asteroid from a far field region to the gateway region, where there is mutual interaction with the second asteroid, which is assumed to be the origin of the relative motion. The second impulse changes the trajectory of the asteroid in the gateway region to a linear drift approaching the second asteroid. The third impulse is calculated by means of increasing the Jacobi integral to reach the critical value required to close the zero-velocity curve. It is demonstrated in principle that the triple impulses enable the candidate asteroids to be captured in a bound pair in Earth's orbit. It is also shown that the thruster on-time for the capture impulse as applied for the different small asteroids considered is short relative to the natural time-scale of the orbital dynamics of the problem, which shows the feasibility of the impulse approximation with the typical thruster forces applied. This strategy could provide a basis for parking small captured near-Earth asteroids in Earth's orbit.

1. Introduction

In recent years, there has been increasing interest in mining and harvesting minerals from near-Earth asteroids (NEAs) that may be rich in ores and raw materials [1]. Due to their risk and proximity to Earth's orbit, NEAs also pose a danger in terms of collision that should be avoided [2–5].

A suggested approach to capturing NEAs would be to trap these asteroids in an orbit around the Earth or at the $L_{4/5}$ Lagrange equilibrium points of the Earth–Moon system. This approach has been previously studied for asteroids that can be captured at the $L_{1/2}$ Lagrange equilibrium points [3]. However, the $L_{1/2}$ points are unstable equilibrium points as opposed to $L_{4/5}$ [6]. Hence, it is of interest to explore capturing NEAs at $L_{4/5}$ or in high Earth orbit. In this pursuit, we need to take into consideration that these smaller asteroids typically do not exist on their own, but rather develop as a rubble pile where all the individual components are held together gravitationally. Therefore, questions related to parking multiple NEAs for a prolonged period in the Earth's orbit, lunar orbit, or $L_{4/5}$ points in the Earth–Moon system form a topic of interest.

One study that focused on NEAs in the Earth–Moon system investigated a new type of lunar asteroid capture [3]. In this type of lunar asteroid capture, the captured asteroid would be given two impulses. The first impulse ensures the asteroid leaves its initial heliocentric orbit. The subsequent impulse inserts the asteroid into the L_2 stable manifold in the Earth–Moon circular restricted three-body problem. Similarly, engineering strategies to capture NEAs have been investigated in Ref. [7] and could therefore be employed to fission binary asteroid pairs after a close encounter with a planetary body. This work allows us to determine capture regions for the minor body of the binary pair by understanding the zero velocity curves for the planar parabolic restricted three-body problem.

Moreover, aerobraking manoeuvres to capture candidate asteroids can have low energy costs [8]. Research has defined two ways of aerobraking and two approaches where the captured asteroid, after the aerobraking manoeuvre, can be injected a bound Earth orbit at the perigee. Furthermore, Ref. [9] studied dismantling the surface material

* Corresponding author.
E-mail addresses: 2471297A@student.gla.ac.uk, aralgethami@kau.edu.sa (A.R. Algethami), colin.mcinnes@glasgow.ac.uk (C. R. McInnes), matteo.ceriotti@glasgow.ac.uk (M. Ceriotti).
[1] PhD candidate, James Watt School of Engineering, James Watt North Building. Permanent; King Abdelaziz University, Lecturer, Astronomy and Space Science Department, Al-Sulaymaniyah campus..
[2] James Watt Chair, Professor of Engineering Science, James Watt School of Engineering, James Watt South Building..
[3] Senior Lecturer, James Watt School of Engineering, James Watt South Building..

https://doi.org/10.1016/j.actaastro.2023.11.006
Received 16 June 2023; Received in revised form 3 November 2023; Accepted 6 November 2023
Available online 11 November 2023

Nomenclature

D	= distance of the Moon from the Earth
d	= distance of the binary asteroids from the Earth
f	= Force of the thruster
G	= centre-of-mass of the asteroids
g	= universal gravitational constant
J	= mechanical impulse for the capture
$L_{1/2}$, $L_{4/5}$	= Lagrange points
lu	= length scale
M_{Earth}	= mass of the Earth
M_{moon}	= mass of the Moon
m_3, m_2	= mass of two asteroids
r	= radius of asteroid
t	= time
tu	= time scale
X, Y	= components of position in inertial frame
$\overline{\rho}$	= density
ξ, η	= components of position in relative frame
$\dot{\xi}, \dot{\eta}$	= components of velocity in relative frame
μ	= mass parameter of the two asteroids
Γ	= Jacobi constant
ρ	= relative distance between the two asteroids
$\Delta\dot{\eta}$	= capture impulse
ω	= angular velocity

Subscripts

e	= event where the capture impulse is applied
equ	= equilibrium points ($L_{1/2}$)
cr	= critical value of Jacobi integral used for capture manoeuver
o	= state at gateway region
p	= initial state for the scenario
impulse	= time for the capture manoeuver

of rotating spherical asteroids using the 'orbital siphon effect' which was investigated analytically. The study is promising with regards to extracting materials from rotating NEAs or rubble pile asteroids, after which the materials can be transferred to a different orbit. Transfer occurs by initiating the orbital siphon effect with a net radial force on a chain that connects a set of surface material payloads.

In the present paper, the research tasks reported have focused on engineering the dynamics of two asteroids in a circular orbit around the Earth to form a bound binary pair by applying a capture impulse when the two asteroids are within a small distance. Prior to this impulse, the paper presents a complete scenario, with two impulses bringing one asteroid from a far field region, using the linear version of Hill's equations, transferring the asteroid to a region near the second asteroid, and altering the motion to be a linear drift to set up the conditions for capture. A related study has investigated whether continuous acceleration might be used to maneuver two asteroids into a bound pair [10]. However, the methodology used in the design of the impulse analysis is quite different from that of the continuous acceleration analysis.

2. Methodology

2.1. Hill's problem

Hill's equations, which provide a mathematical approximation of the restricted three-body problem known as Hill's problem [11], are ideal for describing the orbital motion of satellites of planetary bodies as they can provide a good approximation of the results generated by modelling orbits of the full three-body problem [12]. Furthermore, the equations of motion of Hill's problem can describe two regions for the relative motion of two small bodies around a primary mass, but distant from each other, as well as the bound motion around the centre-of-mass of the two bodies. The former has an approximate analytical solution [13], while the latter can be solved numerically. Several key papers [14–16] have detailed the prominent periodic and non-periodic families of orbits and their stability regions. Other previous papers [17,18] have modelled the motion of binary asteroids as a version of Hill's problem in which the centre-of-mass of the binary asteroid moves in a circular orbit around the Sun. A model describing the centre-of-mass of a binary asteroid system moving on an elliptic orbit has also been formulated [19]. This problem has also been used in spacecraft mission design [20].

The present paper focuses on applying Hill's problem to the problem of asteroid clustering in Earth's orbit. It will be assumed that two small NEAs have been captured in neighbouring circular orbits and that a strategy is required to form a bound binary pair for long-term parking. The issue to be investigated is the gravitational interaction between the

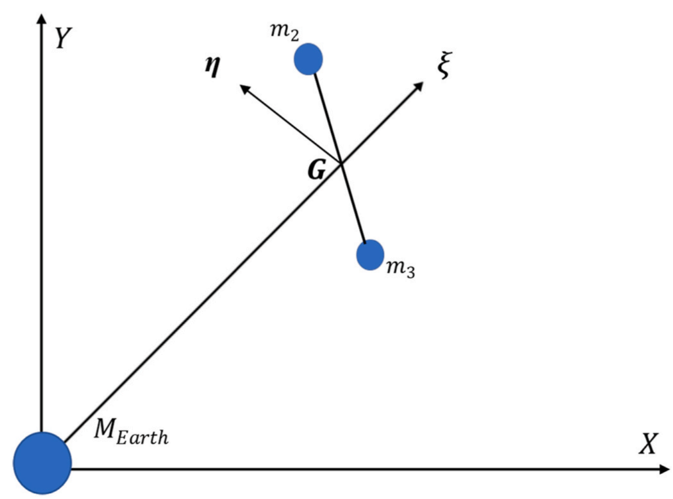

Fig. 1. Definition of the inertial frame (X, Y), where the origin is on the main body, and the rotational frame (ξ, η), where the centre-of-mass is the point G between the two small asteroids.

two small asteroids, when the distance between them is small enough, in principle, to have their quasi-Keplerian motion neglect the force from the central body. A capture impulse from a spacecraft attached to one of the asteroids is assumed to be used to transition to such bound motion. The asteroids of concern in this paper are NEAs with a diameter of 40 m or less that could be captured in a high orbit about the Earth.

2.1.1. Hill's equations

Using the equations of motion for the two small bodies, the dynamics of the NEAs are formulated in Hill variables by Ref. [15]. The relative motion of the three bodies is shown in Fig. 1, where M is the third main body (in this application, the Earth), and m_2, m_3 are the two small bodies. Then (X, Y) is the inertial reference frame, where the main body M is the centre of motion, while (ξ, η) is the rotational frame of reference for relative motion which is defined by the difference in the positions of the small masses. The centre of the relative frame is at G for the relative motion described in Ref. [17]. Hill's equations can be written as:

$$\ddot{\xi} = 2\dot{\eta} + 3\xi - \frac{\xi}{\rho^3} + O\left(\mu^{\frac{1}{3}}\right) \quad (1)$$

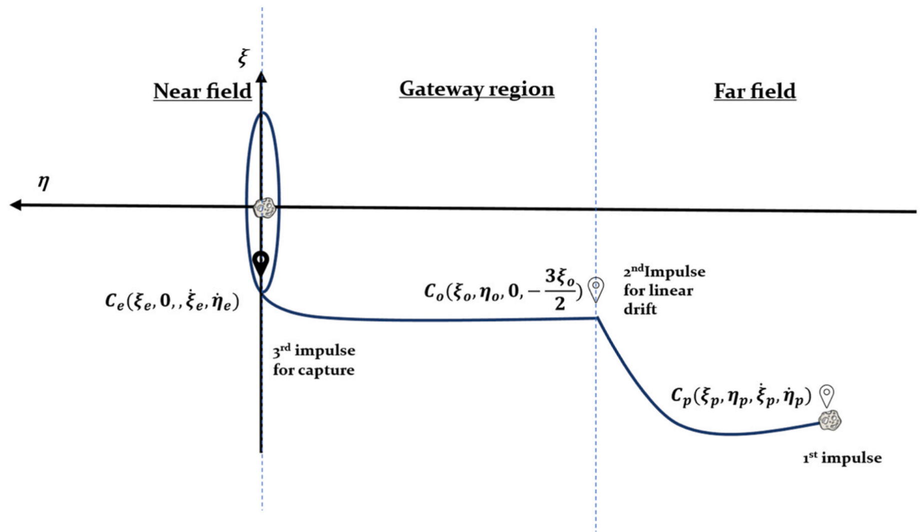

Fig. 2. Triple-manoeuvres scenario to form the binary pair in bound motion. Two impulses transfer the asteroid from the far-field region into the gateway field. The third impulse, at $\boldsymbol{\eta} = \mathbf{0}$, traps the two bodies in their ZVC.

$$\ddot{\eta} = -2\dot{\xi} - \frac{\eta}{\rho^3} + O\left(\mu^{\frac{1}{3}}\right) \tag{2}$$

where $\mu = \frac{m_3}{m_3+m_2}$ is the mass ratio of the problem, and $\rho = \sqrt{\xi^2 + \eta^2}$ is the separation of the two small masses. When ρ is large enough, the gravitational interaction of the two small bodies can be neglected, and Eqs. (1) and (2) will reduce to the linear form:

$$\ddot{\xi} = 2\dot{\eta} + 3\xi \tag{3}$$

$$\ddot{\eta} = -2\dot{\xi} \tag{4}$$

Equations (3) and (4) are known as the Hill-Clohessy-Wiltshire equations. They were initially employed to study the relative motion of satellites orbiting the Earth [21], and subsequently for the purpose of rendezvous and proximity operations. In this instance, they will be used to determine the first impulse applied to the asteroid in the far field region and the second impulse to rendezvous with the second asteroid via the gateway region, defined later. Assuming the initial position and velocity components for the Hill-Clohessy-Wiltshire equations are $\left(\xi_o, \eta_o, 0, -\frac{3\xi_o}{2}\right)$, Section III will show that use of these initial conditions will ensure ξ remains constant while η will exhibit a uniform drift. Due to these equations being linear, they can be solved analytically, again as will be shown later where this behaviour can be verified.

2.2. Jacobi integral

The Jacobi integral is the effective energy constant of motion of the circular restricted three-body problem. For Hill's non-dimensional equations, the Jacobi integral is given by Ref. [15] as:

$$\Gamma = 3\xi^2 + \frac{2}{\sqrt{\xi^2 + \eta^2}} - \dot{\xi}^2 - \dot{\eta}^2 \tag{5}$$

The Jacobi integral allows us to model strategies to capture NEAs [22] by determining the zero-velocity curve (ZVC). The ZVC separates the volume of space where motion is and is not allowed. The strategy has been applied in the Sun–Earth circular restricted three body-problem in Ref. [23] aimed at trapping the candidate asteroid inside a ZVC around the Earth by adjusting Γ with an impulsive manoeuvre. This strategy has also been extended to capture asteroids at the L_1 and L_2 points of the Earth–Moon system [3,4]. Using an implementation of the Jacobi integral permits the analysis of constraints for the change in velocity needed for capture. However, in the present paper, the Jacobi integral will be implemented for a different dynamical model using Hill's equations and, importantly, to serve the objective of clustering of two asteroids in bound motion by an impulse manoeuvre and so capture the two small bodies in the ZVC.

3. Forming an artificial binary pair

In the relative coordinates, it can be considered that one asteroid is located at the origin while the other moves relative to it. As a simple capture strategy, and for potential ease of operational implementation, a capture impulse will now be applied at the crossing of the ξ-axis. Fig. 2 illustrates the required manoeuvres for the full scenario of three impulses.

In Fig. 2, consider applying the third impulse when the motion intersects the $\boldsymbol{\xi}$-axis defined by $\eta = 0$, in the near field area at location $C_e(\xi_e, 0, \dot{\xi}_e, \dot{\eta}_e)$. This is the capture event definition chosen in this paper. This creates a constraint in the dynamics of the problem to ensure that the relative motion of the two bodies will therefore allow them to become bound. The small impulse applied at this event forms a closed zero-velocity curve defining the bound motion. Prior to the capture impulse in the scenario, as shown in Fig. 2, there is a requirement that the relative motion between the two asteroids should comprise a linear drift. Therefore, to ensure that the motion has linear drift, a point $C_o\left(\xi_o, \eta_o, 0, -\frac{3}{2}\xi_o\right)$ is defined in the gateway region. The second impulse will transfer the trajectory to a linear drift from the first impulse designed in far field region $C_p(\xi_p, \eta_p, \dot{\xi}_p, \dot{\eta}_p)$.

Based on the Jacobi constant, to study the constraints noted above, the change in the total effective energy of the system can be found from the event Jacobi constant Γ_e, at the event where the capture impulse is applied, and the critical Jacobi constant required to capture Γ_{cr} and to close the ZVC. At the event coordinates the asteroid position and velocity are defined by $(\xi_e, 0, \dot{\xi}_e, \dot{\eta}_e)$. Thus, Γ_e is defined as:

$$\Gamma_e = 3\xi_e^2 + \frac{2}{\rho_e} - \dot{\xi}_e^2 - \dot{\eta}_e^2 \tag{6}$$

$$\Gamma_e = A - \dot{\xi}_e^2 - \dot{\eta}_e^2 \tag{7}$$

where $A = 3\xi_e^2 + \frac{2}{\rho_e}$ and $\rho_e = |\xi_e|$.

After applying an impulse $\Delta\dot{\eta}_e$ along the η-axis at the capture event, the critical Jacobi constant is defined as:

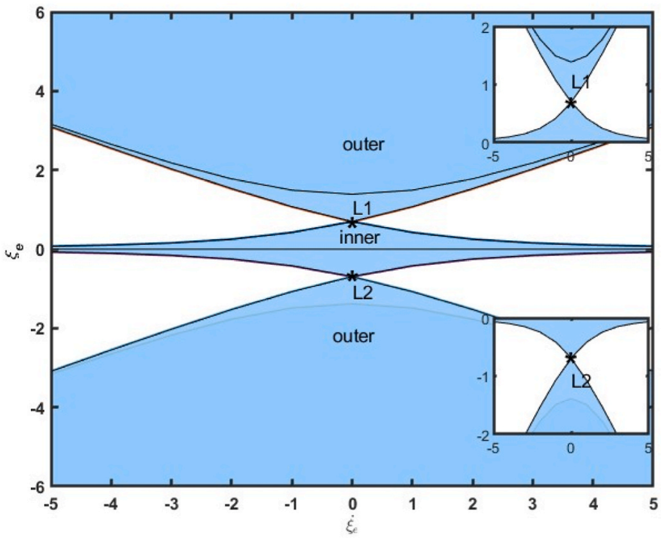

Fig. 3. The analytical solution for inequality in Eq. (**10**). Inner area is between equilibrium points $L_{1/2}$.

$$\Gamma_{cr} = A - \dot{\xi}_e^{\,2} - (\dot{\eta}_e + \Delta\,\dot{\eta})^2 \tag{8}$$

According to this requirement, the impulse $\Delta\dot{\eta}$ is then given by:

$$\Delta\dot{\eta} = \sqrt{-\Gamma_{cr} + A - \dot{\xi}_e^{\,2}} - \dot{\eta}_e \tag{9}$$

in this paper, $\Gamma_{cr} = 4.3269$ is the required critical Jacobi constant to ensure that the ZVC is closed around the captured binary pair of asteroids. It is found by substituting the location of the collinear Lagrange points in Eq. (5) which yields the critical Jacobi integral. The Lagrange points are the equilibrium points where the total force, comprised of the tidal force from the main body and the gravitational force between the asteroids, is equal to zero. These points are calculated by using Eqs. (1) and (2), where $\dot{\xi} = \dot{\eta} = \ddot{\xi} = \ddot{\eta} = 0$ and L_1 and L_2 are therefore located at $\eta_{equ} = 0$, $\xi_{equ} = \pm\left(\frac{1}{3}\right)^{\frac{1}{3}}$. Then, to ensure that the interaction between the two bodies continues after capture, they should be trapped within the ZVC where the Jacobi constant is not less than Γ_{cr}.

It is important to remark that the stability of planar orbits in Hill's equations is valid when considering low inclinations, due to the oscillatory type of out-of-plane motion explained in Ref. [17]. Thus, as we introduce only small changes in transverse velocity within the capture area, between the equilibrium points L_1 and L_2, such planar stability should not be affected, and Eq. (8) should be valid for the planar scenario here. Now that the capture impulse required to close the ZVC and ensure bound motion of the binary asteroid pair has been determined, the constraints on such a manoeuvre will be considered.

3.1. *Constraints on the capture manoeuvre*

Equation (9) will now be used to calculate the real-valued impulse $\Delta\dot{\eta}$ required to close the ZVC. However, Eq. (9) must have a constraint on the expression under the root to avoid a complex value. Therefore, it can be noted that:

$$3\xi_e^2 + \frac{2}{\rho_e} - \dot{\xi}_e^2 - \Gamma_{cr} > 0 \tag{10}$$

This inequality provides the maximum value for $\dot{\xi}_e$ to ensure that the calculation for $\Delta\dot{\eta}$ produces a real value, and hence, the capture manoeuvre is possible.

Prior to describing the capture manoeuvre in detail, Eq. (**10**) is solved for ξ_e by using Cardano's formula for a cubic equation [24]. The solution indicates the area of the inequality and shows all possible values for $\xi_e, \dot{\xi}_e$ at the event which have a real value for $\Delta\dot{\eta}$, as shown in Fig. 3. The solution's critical values can be found by setting $\dot{\xi} = 0$, corresponding to the L_1 and L_2 points.

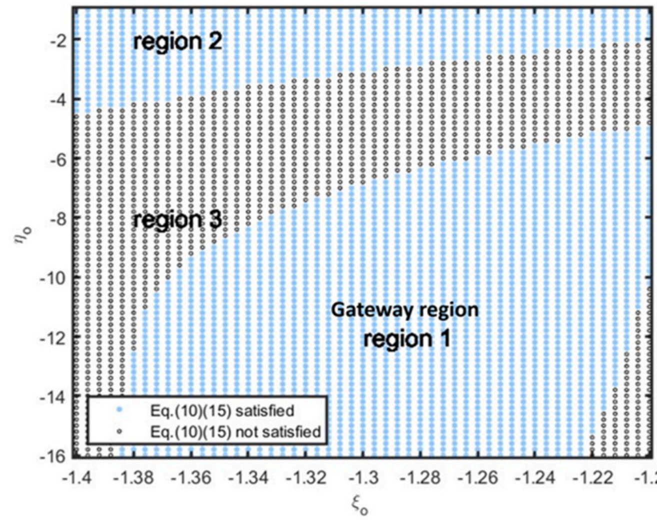

Fig. 4. Grid of initial values $(\boldsymbol{\xi}_o, \boldsymbol{\eta}_o, \mathbf{0}, -3\boldsymbol{\xi}_o/\mathbf{2})$ produced by analysing constraints Eqs. (10) and (15). Region 1 successful capture manoeuvre; region 2 velocity constraints valid, but two asteroids not in their Hill sphere; region 3 non-capture manoeuvre.

3.1.1. *Solving the inequality for* ξ

In Fig. 3, the event at $\eta = 0$ can be used for a capture manoeuvre if $(\xi_e, \dot{\xi}_e)$ is within the shaded diamond-shape region (inner area). Thus, the manoeuvre at the event occurs between L_1 and L_2, so the outer shaded area cannot be used for capture. This result aligns with Ref. [14] in relation to escape trajectories when $(\xi_e, \dot{\xi}_e)$ is located in the outer areas. From Eq. (9), $\Delta\dot{\eta}$ defines the capture manoeuvre and is dependent on the two terms of the velocity components at the capture event. The first constraint where $\eta_e = 0$ is retrieved from Eq. (10) for $\dot{\xi}_e$, and stated in Eq. (11). The second constraint for $\dot{\eta}_e$ will be considered later:

$$A - \Gamma_{cr} > \dot{\xi}_e^2 \tag{11}$$

where again $A = 3\xi_e^2 + \frac{2}{|\xi_e|}$, and A can be considered as the effective potential energy at the event. Thus, Eq. (11) depicts the constraints on $\dot{\xi}_e$. Next, we will consider the constraints on $\dot{\eta}_e$.

Initially, we start with the value of Γ_e at the capture manoeuvre event:

$$\Gamma_e = 3\xi_e^2 + \frac{2}{|\xi_e|} - \dot{\xi}_e^2 - \dot{\eta}_e^2 \tag{12}$$

$$\dot{\xi}_e^2 = A - \Gamma_e - \dot{\eta}_e^2 \tag{13}$$

By using Eq. (11), it can be observed that:

$$A - \Gamma_e - \dot{\eta}_e^2 < A - \Gamma_{cr} \tag{14}$$

which then implies:

$$\dot{\eta}_e^2 > \Gamma_{cr} - \Gamma_e \tag{15}$$

Equation (15) gives the minimum value required for $\dot{\eta}_e$ that is related to the Jacobi integral Γ_{cr} to design the capture manoeuvre. For a more practical use of Eq. (15), we can use the conservation of the Jacobi integral over the approach trajectory, then $\Gamma_e = \Gamma_0$, where Γ_0 is the Jacobi integral at the initial starting point of the capture manoeuvre C_o at the edge of the gateway region, as shown in Fig. 2, so that:

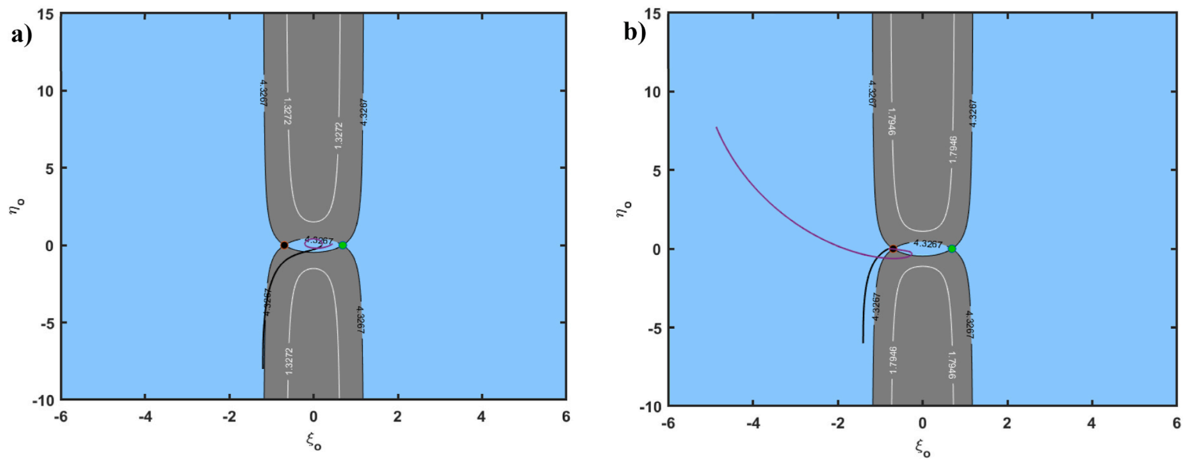

Fig. 5. Two examples of the trajectories after the final capture manoeuvre: (a) captured for initial condition chosen from region 1. (b) non-captured for initial condition from region 2. $\boldsymbol{L_1}$ and $\boldsymbol{L_2}$ points denoted by black and green dots. (For interpretation of the references to colour in this figure legend, the reader is referred to the Web version of this article.)

$$\dot{\eta}_e^2 > \Gamma_{cr} - \Gamma_0 \tag{16}$$

Equations (11) and (16) are constraints on the value of the velocity components at the event where the impulse is applied to change the asteroid's energy. It can be noted that $\dot{\xi}_e^2$ has a maximum value, whereas $\dot{\eta}_e^2$ has a minimum value. Both are related to the Jacobi integral Γ_{cr} required to close the ZVC and ensure the motion is bounded. It is assumed that the initial relative motion at C_o between the two asteroids will comprise a linear drift, as noted in Fig. 2, so that at the point C_o, the asteroid position and velocity components are given by $\left(\xi_o, \eta_o, 0, -\frac{3}{2}\xi_o\right)$. The full scenario in subsection IIIb will provide more detail about maneuvering the asteroids to be in a linear drift state.

These two constraints are now shown in Fig. 4. The blue area defined by region 1 in Fig. 4 is produced by the constraints in Eq. (16) and Eq.

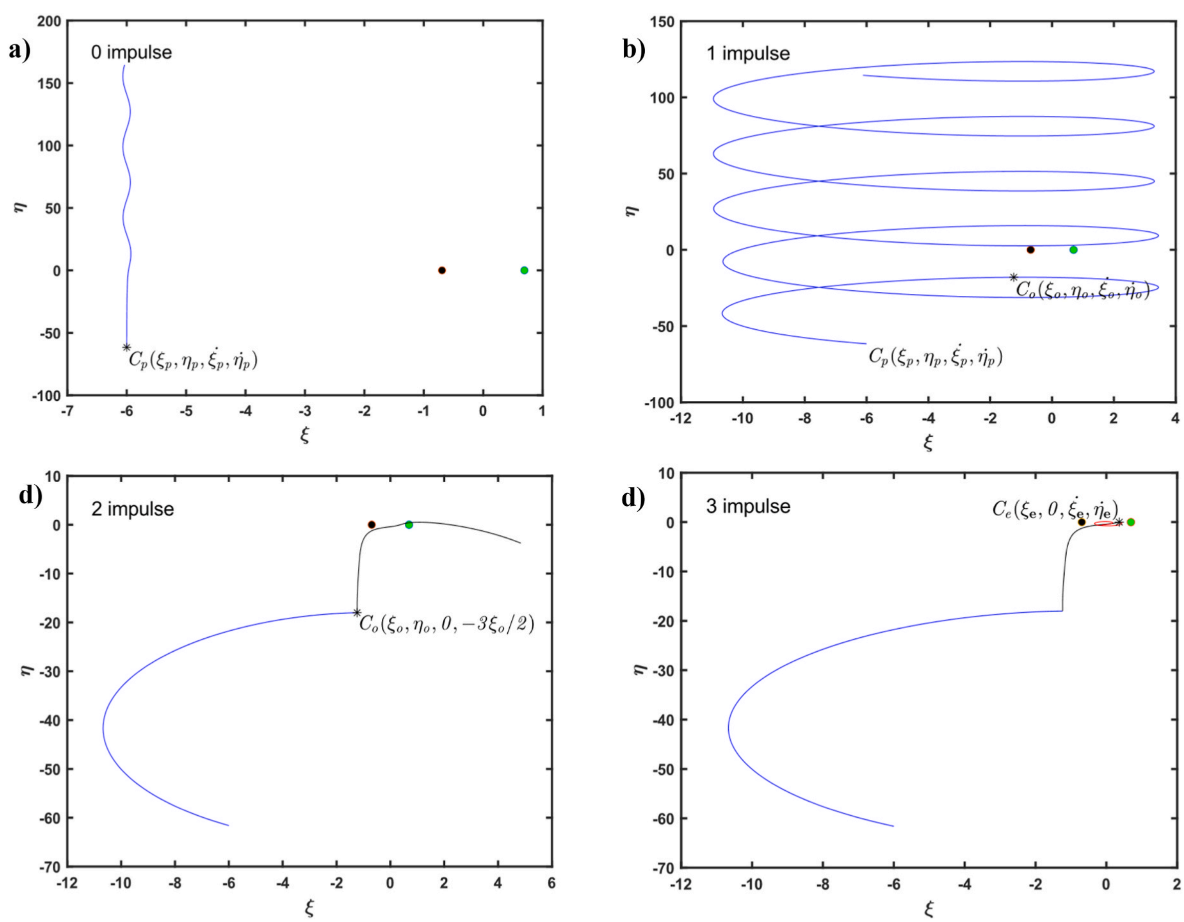

Fig. 6. Full scenario of three impulses. The two dots represent $\boldsymbol{L_{1/2}}$, difference in colour of the trajectory represents the impulses. (a) no impulse applied. (b) first impulse directing the trajectory to initial position in gateway region. (c) second impulse fixing velocity components to be $(\mathbf{0}, -\mathbf{3}\boldsymbol{\xi_o}/\mathbf{2})$. (d) third capture impulse applied at $(\boldsymbol{\xi_o}, \mathbf{0})$. (For interpretation of the references to colour in this figure legend, the reader is referred to the Web version of this article.)

(11). It thus represents the possible initial values that lead to capture of the two asteroids in a closed ZVC and as noted, is named here the gateway region. In region 2, the initial values satisfy the constraints in Eq. (16) and Eq. (11) but not the constraints on the event location noted in Fig. 3 (the capture event location should be between L_1 and L_2). For region 3, which is represented with grey dots, the constraints in Eq. (16) and Eq. (11) are not valid, which means the initial velocity components for the asteroid are not capable of reaching the capture event to apply an impulse.

Fig. 5 shows examples of capture manoeuvre and non-capture manoeuvre from different regions of Fig. 4. For these examples, the initial parameters for the capture manoeuvre are $\xi_o = -1.22$ and $\eta_o = -8$, whereas in relation to the non-capture manoeuvre, the initial parameters are $\xi_o = -1.5$ and $\eta_o = -6$. The figures demonstrate a grey region denoting the ZVC, which is closed after adding the impulse to reach Γ_{cr}. In addition, the white contour lines show the Jacobi integral before adding the impulse, so the ZVC is open before the impulse.

3.2. Full capture scenario

As noted earlier, prior to the capture manoeuvre, two further manoeuvres can be considered to transfer the asteroid to the gateway region. These manoeuvres bring the asteroid into this region with relative initial conditions that ensure the uniform drift of the asteroid towards the origin as required for capture. The initial values of the velocity components are then again in the form $(\xi_0, \eta_0, \dot{\xi}_0, \dot{\eta}_0) = (\xi_0, \eta_0, 0, -\frac{3}{2}\xi_0)$. We assume that prior to reaching the gateway region the initial conditions are $(\xi_p, \eta_p, \dot{\xi}_p, \dot{\eta}_p)$ at point C_p, as shown in Fig. 2. Then, using the solution of Eq. (3) and Eq. (4) that was found in a state vector δs where $\delta s^T = [\delta r^T \delta v^T] = [\xi\ \eta \dot{\xi} \dot{\eta}]$, the 4×4 state transition matrix can be defined as in Ref. [25]:

$$\delta s = Q(t)\delta S(0) \tag{17}$$

where $Q(t)$ is assembled from the coefficients of the solution, which can be written as:

$$Q(t) = \begin{bmatrix} M(t) & N(t) \\ S(t) & T(t) \end{bmatrix} \tag{18}$$

and where the matrices are defined by:

$$M(t) = \begin{bmatrix} 4 - 3\cos t & 0 \\ 6(\sin t - t) & 1 \end{bmatrix} \tag{19}$$

$$N(t) = \begin{bmatrix} \sin t & -2(1 - \cos t) \\ -2(1 - \cos t) & 4\sin t - 3t \end{bmatrix} \tag{20}$$

$$S(t) = \begin{bmatrix} 3\sin t & 0 \\ -6(1 - \cos t) & 0 \end{bmatrix} \tag{21}$$

$$T(t) = \begin{bmatrix} \cos t & 2\sin t \\ -2\sin t & 4\cos t - 3 \end{bmatrix} \tag{22}$$

The position and relative velocity can then be written as:

$$\delta r(t) = M(t)\delta r(0) + N(t)\delta v(0) \tag{23}$$

$$\delta v(t) = S(t)\delta r(0) + T(t)\delta v(0) \tag{24}$$

To perform the first manoeuvre, it will be assumed that in the far field region the asteroid has initial conditions $(\delta r(0), \delta v(0)) = (\xi_p, \eta_p, \dot{\xi}_p, \dot{\eta}_p)$, as noted in Fig. 3. Then, Eqs. (23) and (24) can be used to determine the first impulse required for the asteroid to reach the desired position and velocity components $(\delta r(t), \delta v(t)) = (\xi_o, \eta_o, \dot{\xi}_o, \dot{\eta}_o)$ at the gateway region. A second impulse then ensures that the motion will have linear drift with $(\xi_0, \eta_0, 0, -\frac{3}{2}\xi_0)$, as shown in Fig. 6.

Fig. 6 illustrates the scenario of three impulsive manoeuvres. The initial parameters $(\xi_p, \eta_p, \dot{\xi}_p, \dot{\eta}_p)$ for linear drift trajectories can be seen in Fig. 6a. With no impulse applied, the trajectory remains linear until the asteroid reaches the near field region. Hence, the gravitational interaction with these initial values in the far field region is negligible. Fig. 6b shows that, at the transfer to the gateway region within a transfer time of half an orbit, the position of this point is selected as $(\xi_o, \eta_o) = (-1.3, -10)$ to be targeted by the first impulse. Then, the second impulse achieves the relative velocities for linear drift within the gateway region such that $(\dot{\xi}_o, \dot{\eta}_o) = (0, -\frac{3}{2}\xi_0)$. Finally in Fig. 6d at $\eta = 0$, at the event location $(\xi_e 0, \dot{\xi}_e, \dot{\eta}_e)$, the manoeuvre defined by Eq. (9) is applied to change the Jacobi constant to that required for bound relative motion within a closed ZVC.

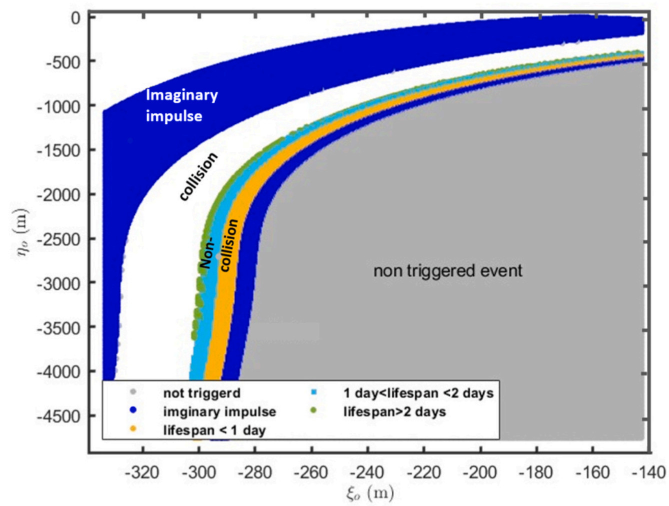

Fig. 7. Dimensional gateway region to manoeuvre two asteroids with 15 m radius.

4. Operational analysis: Case study

4.1. Assumptions and input parameters

By retaining physical dimensions to the system, Eqs. (1) and (9) can be modified by using the length scale $lu = \left(\frac{\mu}{\omega}\right)^{\frac{1}{3}}$ and time scale $tu = \left(\frac{1}{\omega}\right)$, where the mass ratio $\mu = \frac{m_3}{m_3 + m_2}$, and $\omega^2 = g\frac{M_{Earth}}{d^3}$, where d ($1.125027 \times 10^8\ m$) is the distance of the binary pair of asteroids from the Earth, g ($6.67430 \times 10^{-11}\ m^3\ kg^{-1}\ s^{-2}$) is the universal gravitational constant, and M_{Earth} ($5.9742 \times 10^{24}\ kg$) is the mass of the Earth.

The grid in Fig. 7 is produced considering two asteroids, assumed to be uniform spheres, which are now assumed to have a radius of r(15 m), density $\overline{\rho}$ ($2 \times 10^3\ kgm^{-3}$), and at a distance of 0.3 of the Earth–Moon distance. In addition, one asteroid is again assumed to be at the origin of the relative coordinates of the problem. The dimensional grid in Fig. 7 now exhibits different features to the gateway initial values. During the numerical integration of Hill's equation, a collision detection algorithm is implemented, such that the simulation stops when a collision is detected. Implementation of this algorithm forces consideration of the lifespan of the binary asteroid before collision. Given the slow relative velocities, a largely inelastic collision is likely to result in the pair of asteroids remaining in contact to form abound cluster.

4.2. Results and discussion

The dimensional gateway region is now separated into two regions. The first region is the collision region, the region of initial values in the gateway that results in the two asteroids colliding prior to the capture event chosen in Section III. The second region consists of non-colliding

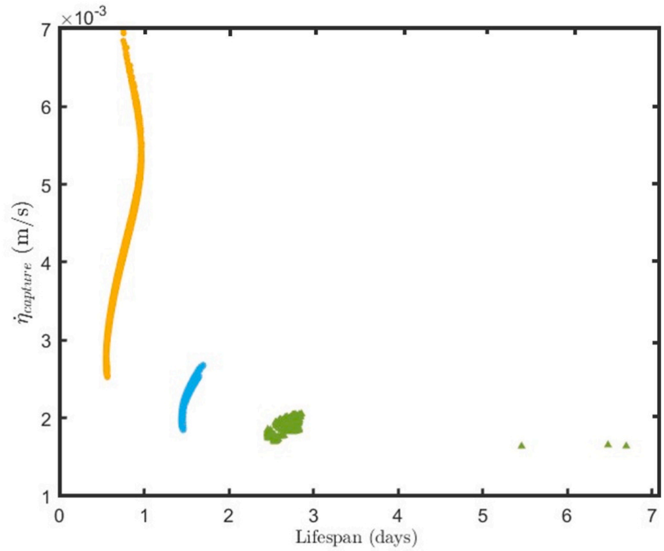

Fig. 8. Comparing $\Delta\dot{\eta}_{capture}$ versus timespan for the captured asteroid pairs. Dots represent initial values from the gateway region in Fig. 7.

trajectories. In this region, after the third capture impulse, they do not collide for a finite time.

Fig. 7 shows changes in the initial value region that resulted in capturing the asteroid within the ZVC, depicted as region 1 in Fig. 4. The changes are due to retaining physical units in the numerical integration and considering the finite size of the NEAs. Fig. 7 shows a collision region in the white area which has initial values developing trajectories that collide before reaching the capture event at $\eta = 0$ (ξ-axis). In addition, the grid in Fig. 7 shows the same result for non-triggered events, depicted in grey, from the initial values. This result aligns with the results in Fig. 4. Initial values from the non-triggered event region produce trajectories which are not capable of reaching the capture event at $\eta = 0$. The blue areas also depict initial values of trajectories where the velocity components at the event do not satisfy the constraints in Eq. (11) and Eq. (16). In addition, there is a narrow region of initial conditions between the non-triggered and collision area, represented in three marker colours. This area defines non-collision trajectories that reach the event and have a real-valued capture impulse that closes the ZVC around the binary asteroid pair. It should be pointed out that even if the capture impulse is added only to one asteroid, Hill's equations allow for the coupling of their dynamics. It can be established that despite the asteroid's center-of-mass dynamics being perturbed by the impulses, Hill's equations still adequately represent their relative motion.

Furthermore, the coloured markers for the non-collision area in Fig. 7 differ for each of the three lifespans of the binary asteroids considered here. Orange denotes the initial values for developing a captured binary pair with a lifetime of one day before collision. Light blue denotes the initial values for an asteroid pair with a lifespan greater than one day and less than two days. Green denotes the initial values for the longest binary pair, a pair that lasts more than two days before collision. The representation shows that the difference in lifespan is determined by the location of initial conditions. This lifespan calculation is obtained by stopping the simulation at a relative distance between the asteroids of 30 m of the sum of the radius of both asteroids. The lifespan versus the required capture impulse $\Delta\dot{\eta}_{\text{capture}}$, as shown in Fig. 8, is for the initial values in the non-collision region shown in Fig. 7. Fig. 8 demonstrates that the captured asteroids have a longer lifespan before collision, more than two days, when the impulse $\Delta\dot{\eta}_{\text{capture}}$ is smaller. Likewise, the minimum lifespan for binary asteroid dynamics, within the closed ZVC, is less than one day when the impulse $\Delta\dot{\eta}_{\text{capture}}$ value is larger. The capture impulse is seen to be small, as expected for small NEAs.

Furthermore, Fig. 8 indicates the magnitude of $\Delta\dot{\eta}_{capture}$ for all initial conditions in the non-collision area which is of order $10^{-3}\ ms^{-1}$. We can assume now that a small thruster provides a force of $f = 1000N$, and consider the density for stony and metallic asteroids and the radius of the small spherical uniform asteroids. Then, the mechanical impulse J required for capture is the product of the asteroid mass and $\Delta\dot{\eta}_{capture}$. For a typical case considered the impulse could reach 3×10^4 Ns, and so the time for the manoeuver can be estimated as $\Delta t_{impulse} = \frac{J}{f} \approx 30s$. This suggests the capture impulse is short compared to the time scale of the dynamics of the problem, again given by $tu = \left(\frac{1}{\omega}\right) = 5.98\times10^4 s$. Table 1 seeks to examine a range of realistic mean values for $\Delta\dot{\eta}_{capture}, J$ and $\Delta t_{impulse}$. The mean of $\Delta\dot{\eta}_{capture}$ in Table 1 is the sum of all $\Delta\dot{\eta}_{capture}$ for captured initial values in the gateway region divided by the number of initial values propagated for different mass values at Table 1. The mass of the spherical asteroids is computed by approximate values of the density for stony $(2\times10^3 kg/m^3)$ and metallic $(6\times10^3 kg/m^3)$ asteroids and the assumed asteroid radii in Table 1. Subsequently, J and $\Delta t_{impulse}$ are found based on mean of $\Delta\dot{\eta}_{capture}$. Table 1 illustrates that the capture impulse approximation is appropriate as the values of $\Delta t_{impulse}$ are small in comparison of the time scale of the dynamics of the problem.

As previously noted, the location of the capture orbit is between the Earth and the Moon, however the Hill radius $\boldsymbol{R_H}$, is defined as:

$$R_H = D\sqrt[3]{\frac{M_{moon}}{3M_E}} \tag{25}$$

where D represents the distance between Earth and the Moon, and it is equal to 3.75009×10^8 m. The ratio of the mass of Moon to the mass of the Earth is approximately $1/81$ from Ref. [26], so that $R_H = 0.16D$. As it was specified in subsection IVa, the distance of the captured asteroids from the centre of the Earth is assumed to be $d = 0.3D$. It is clear therefore that the asteroids are far from the influence of lunar gravitational perturbations.

5. Conclusion

The proposed strategy uses Hill's equations to capture two NEAs far from each other in a bound binary pair by applying a three-impulse-

Table 1
Different asteroid masses for different radii and density, and approximation for $\Delta\dot{\eta}_{capture}, J, \Delta t_{impulse}$.

Asteroid radius (m)	Density (kgm^{-3})	Mass (kg)	Mean of $\Delta\dot{\eta}_{capture}$ (ms^{-1})	$J(Ns)$	$\Delta t_{impulse}(s)$	$\frac{\Delta t_{impulse}}{tu}$
20	2×10^3	6.70×10^7	$\sim 10^{-3}$	6.70×10^4	67	1.12×10^{-3}
	6×10^3	2.01×10^8	$\sim 10^{-3}$	2.01×10^5	201	3.36×10^{-3}
15	2×10^3	2.83×10^7	$\sim 10^{-3}$	2.83×10^4	28	4.69×10^{-4}
	6×10^3	8.48×10^7	$\sim 10^{-3}$	8.48×10^4	84	1.41×10^{-3}
10	2×10^3	8.48×10^6	$\sim 10^{-4}$	8.48×10^2	0.85	1.42×10^{-5}
	6×10^3	2.51×10^7	$\sim 10^{-3}$	2.51×10^4	25	4.18×10^{-4}
5	2×10^3	1.05×10^6	$\sim 10^{-4}$	1.05×10^2	0. 1	1.67×10^{-5}
	6×10^3	3.14×10^6	$\sim 10^{-4}$	3.14×10^3	3	5.02×10^{-5}

manoeuvre sequence. Bringing the first asteroid to a gateway region to undertake gravitational interaction with the second asteroid is accomplished by using the linearized form of Hill's equations. A second impulse alters the relative velocity components to induce the asteroid being maneuvered into a linear drift. A third impulse is subsequently employed to increase the Jacobi integral of Hill's equations to close the ZVC. The results indicate that the strategy leads to the capture of two asteroids in bound orbits around the Earth. The results further indicate the importance of defining the gateway region using constraints on the asteroid velocity prior to capture. These constraints are then analysed later in dimensional units, where the asteroids are assumed to have a spherical form with a radius of 15 m. This analysis produces a narrower gateway region that prevents a collision prior to the final capture impulse. The classification for the lifespan of the resulting binary pair of asteroids is presented in terms of the initial conditions at the gateway region. The paper has shown that initiating the motion in the gateway region offers a longer lifespan and lower impulse for the captured bound binary pair. Furthermore, the short thruster on-time for the capture impulse for various small asteroid radii and densities shows that such an impulse approximation is appropriate under typical thruster forces.

Declaration of competing interest

The authors declare that they have no known competing financial interests or personal relationships that could have appeared to influence the work reported in this paper.

Acknowledgments

Amirah R. Algethami was supported by a scholarship from King Abdul-Aziz University, Deanship of Scientific Research in Saudi Arabia. Colin R. McInnes was supported by a Royal Academy of Engineering in the United Kingdom through the Chairs in Emerging Technologies scheme. For the purpose of open access, the author(s) has applied a Creative Commons Attribution (CC-BY) licence to any Author Accepted Manuscript version arising from this submission.

References

[1] Z. Hasnain, C.A. Lamb, S.D. Ross, Capturing near-Earth asteroids around Earth, Acta Astronaut. 81 (No. 2) (2012) 523–531, https://doi.org/10.1016/j.actaastro.2012.07.029.

[2] C.R. Chapman, The Hazard of near-Earth asteroid Impacts on Earth, Earth Planet Sci. Lett. 222 (No. 1) (2004) 1–15, https://doi.org/10.1016/j.epsl.2004.03.004.

[3] M. Tan, C. McInnes, M. Ceriotti, Direct and Indirect capture of near-Earth asteroids in the Earth–Moon system, Celestial Mech. Dyn. Astron. 129 (No. 1) (2017) 57–88, https://doi.org/10.1007/s10569-017-9764-x.

[4] H. Urrutxua, D. Scheeres, C. Bombardelli, J.L. Gonzalo, J. Pelaez, What Does it take to capture an asteroid? A case study on capturing asteroid 2006 RH120, Adv. Astronaut. Sci. 152 (2014) 1117–1136.

[5] X. Zhou, X. Li, Z. Huo, L. Meng, J. Huang, Near-Earth Asteroid Surveillance Constellation in the Sun-Venus Three-Body System, vol. 2022, Space: Science & Technology, 2022, https://doi.org/10.34133/2022/9864937.

[6] E. Belbruno, M. Gidea, F. Topputo, Weak stability boundary and Invariant manifolds, SIAM J. Appl. Dyn. Syst. 9 (No. 3) (2010) 1061–1089, https://doi.org/10.1137/090780638.

[7] X. Liu, C. McInnes, M. Ceriotti, Strategies to engineer the capture of a Member of a binary asteroid pair using the planar parabolic restricted three-body problem, Planet. Space Sci. 161 (2018) 5–25, https://doi.org/10.1016/j.pss.2018.05.018.

[8] M. Tan, C. McInnes, M. Ceriotti, Capture of small near-Earth asteroids to Earth orbit using aerobraking, Acta Astronaut. 152 (2018) 185–195, https://doi.org/10.1016/j.actaastro.2018.08.007.

[9] A. Viale, C. McInnes, M. Ceriotti, Analytical Mechanics of asteroid Disassembly using the orbital siphon effect, Proc. R. Soc. A 474 (No. 2220) (2018), 20180594, https://doi.org/10.1098/rspa.2018.0594.

[10] A. Algethami, C.R. McInnes, M. Ceriotti, "Guiding asteroids to form an artificial bound binary pair using continuous control acceleration,", in: Presented at the 74th International Astronautical Congress (IAC), paper code: IAC-23,C1,3,6, x78344, Baku, Azerbaijan, 2023.

[11] G.W. Hill, Researches in the lunar theory, Am. J. Math. 1 (No. 1) (1878) 5–26, https://doi.org/10.2307/2369430.

[12] M. Lara, J.F. Palacián, Hill problem analytical theory to the order Four: application to the computation of Frozen orbits around planetary satellites, Math. Probl Eng. 2009 (2009) 1–18, https://doi.org/10.1155/2009/753653.

[13] M. Hénon, J.-M. Petit, Series Expansions for encounter-type solutions of Hill's problem, Celestial Mech. 38 (No. 1) (1986) 67–100, https://doi.org/10.1007/BF01234287.

[14] M. Henon, Numerical Exploration of the restricted problem. VI. Hill's case: non-periodic orbits, Astron. Astrophys. 9 (1970) 24–36.

[15] J.-M. Petit, M. Henon, Satellite encounters, Icarus 66 (No. 3) (1986) 536–555, https://doi.org/10.1016/0019-1035(86)90089-8.

[16] M. Hénon, New families of periodic orbits in Hill's problem of three bodies, Celestial Mech. Dyn. Astron. 85 (No. 3) (2003) 223–246, https://doi.org/10.1023/A:1022518422926.

[17] B. Chauvineau, F. Mignard, Dynamics of binary asteroids: I. Hill's case, Icarus 83 (No. 2) (1990) 360–381, https://doi.org/10.1016/0019-1035(90)90073-I.

[18] B. Chauvineau, F. Mignard, Generalized Hill's problem - Lagrangian Hill's case, Celestial Mech. Dyn. Astron. 47 (1990) 123–144.

[19] M. Moons, F. Delhaise, E. Depaepe, Elliptical Hill's problem (large and small Impact parameters), Celestial Mech. 43 (1988) 349–359, https://doi.org/10.1007/BF01234579.

[20] B.F. Villac, Dynamics in the Hill Problem with Applications to Spacecraft Maneuvers, 2003.

[21] J.E. Prussing, B.A. Conway, Orbital Mechanics, Oxford University Press, USA, 1993.

[22] X. Liu, C. McInnes, M. Ceriotti, Strategies to engineer the capture of a Member of a binary asteroid pair using the planar parabolic restricted three-body problem, Planet. Space Sci. 161 (2018) 5–25, https://doi.org/10.1016/j.pss.2018.05.018.

[23] H.-X. Baoyin, Y. Chen, J.-F. Li, Capturing near Earth Objects, Res. Astron. Astrophys. 10 (No. 6) (2010) 587–598, https://doi.org/10.1088/1674-4527/10/6/008.

[24] W.S. Anglin, J. Lambek, The cubic and Quartic equations, in: W.S. Anglin, J. Lambek (Eds.), The Heritage of Thales, Springer, New York, NY, 1995, pp. 133–137, https://doi.org/10.1007/978-1-4612-0803-7_26.

[25] J.E. Prussing, B.A. Conway, Orbital Mechanics, Oxford University Press, New York, 1993.

[26] Moon Fact Sheet, Retrieved, https://nssdc.gsfc.nasa.gov/planetary/factsheet/moonfact.html. (Accessed 13 October 2023).